IEEE Access
Multidisciplinary | Rapid Review | Open Access Journal

Received February 28, 2020, accepted March 10, 2020, date of publication March 16, 2020, date of current version March 26, 2020.

Digital Object Identifier 10.1109/ACCESS.2020.2980935

Complexity Analysis and Synchronization Control of Fractional-Order Jafari-Sprott Chaotic System

GUOHUI LI, XIANGYU ZHANG, AND HONG YANG
School of Electronic Engineering, Xi'an University of Posts and Telecommunications, Xi'an 710121, China
Corresponding authors: Guohui Li (lghcd@163.com) and Hong Yang (uestcyhong@163.com)

This work was supported by the National Natural Science Foundation of China under Grant 51709228.

ABSTRACT Aiming at the complexity problem of fractional-order Jafari-Sprott chaotic system, in this paper, Adomian decomposition method is used to study its numerical analysis and a complexity analysis method of fractional-order Jafari-Sprott chaotic system based on fuzzy entropy algorithm, sample entropy algorithm and dispersion entropy algorithm is proposed. For the synchronization and control of fractional-order Jafari-Sprott chaotic system, sliding mode control is used to achieve synchronization of fractional-order Jafari-Sprott chaotic system and a control method of fractional-order Jafari-Sprott chaotic system is proposed based on frequency distribution model of fractional-order integral operator. The main results are as follows: (1) The complexity of the fractional-order Jafari-Sprott chaotic system is greater than the integer-order Jafari-Sprott chaotic system, and fractional-order chaotic system has better application prospects. (2) Moreover, it is concluded that the effect of the dispersion entropy algorithm on detecting complexity is the best, which provides theoretical and experimental basis for the practical engineering application of the fractional-order Jafari-Sprott chaotic system. (3) Synchronization and control of fractional-order Jafari-Sprott chaotic system is accomplished by sliding model control and frequency distribution model of fractional-order integral operator respectively. In particular, the control effect of each variable is accomplished by designing a control law based on the frequency distribution model of fractional integral operator.

INDEX TERMS Fractional-order chaotic system, Adomian decomposition method, complexity analysis, sliding mode control, frequency distribution model of fractional-order integral operator.

I. INTRODUCTION

Research on complexity is involved in various fields. So far there is no unified concept of complexity. Complexity refers to metric value, which has comparative significance, and different complexity algorithms characterize different aspects of complexity. Horgan [1] pointed out that there are multiple definitions of complexity, such as time complexity, space complexity, semantic complexity, Kolmogorov complexity, etc. There are multiple algorithms for calculating complexity. Lempel and Ziv [2] proposed Lempl-Ziv algorithm. Pincus [3] and Sun *et al.* [4] proposed an approximate entropy algorithm. Chen *et al.* [5] and Sun *et al.* [6] proposed a fuzzy entropy algorithm. Larrondo *et al.* [7] and Sun *et al.* [8] proposed a strength statistics algorithm. Azad *et al.* [9] proposed a symbolic entropy algorithm. At present, there are spectral entropy algorithm [10], wavelet entropy algorithm [11] and C_0 algorithm [12] based on Fourier transform and wavelet transform. In addition, complexity algorithms based on entropy are often used in biological and medical research. Yang and Liao [13] applied approximate entropy to the comparison of heart rate between children with sudden infant death and normal children. Lake *et al.* [14] used sample entropy to analyze the change of newborn heart rate signal as the basis for diagnosis of neonatal sepsis. Liu *et al.* [15] used sample entropy to study the electroencephalography (EEG) during sleep, and distinguished the different stages of sleep through the change of sample entropy value. Yang *et al.* [16] analyzed depression by using sample entropy. It can be seen that entropy can be used to test the complexity of various systems. Fractional-order chaotic system is widely used because of its rich dynamic behavior, especially related to complexity. The complexity of fractional-order chaotic system analysis by fuzzy entropy algorithm, sample entropy algorithm and dispersion entropy algorithm has not been reported, so it is necessary to carry out this research.

The associate editor coordinating the review of this manuscript and approving it for publication was Di He.

The current synchronization control methods commonly used in chaotic system research are OGY (firstly proposed by E. Ott, C. Grebogi, J. A. Yorke) control method [17], drive response control method [18], [19], linear and nonlinear feedback control method [20], [21], real-delay feedback control method [22], linear error feedback control method [23], generalized synchronous control method [24], neural network control method [25], [26]. With the deepening research of scientists, a large number of methods have been proposed, such as self-adaptive synchronization method [27], active control synchronization method [28], [29], variable structure synchronization control method [30], [31], fuzzy control synchronization method [32], [33], synchronization method based on state observer [34], coupled synchronization method [35]–[38], etc. Scholars at home and abroad have also achieved some achievements. Mao [39] and Mao and Li [40] studied the synchronization problem of the fractional-order Duffing system with a new approach law and the synchronization control problem of the fractional-order Genesio-Tesi chaotic system. Based on the nonlinear sliding mode integral control method, the control problem of a class of systems has been studied and the proportional integral control method has been widely used in the field of cybernetics [41]. Based on proportional integral control, an accurate tracking and guidance method has been studied, and sliding mode control method has also been widely used in control field [42]. Xu *et al.* [43] studied on sliding mode control for a class of chaotic systems. Aghababa and Akbari [44] studied the control synchronization of two types of chaotic systems with uncertain disturbances and designed an appropriate sliding mode controller and adaptive rate to eliminate the effects of system uncertainty and external disturbances, and finally achieved system synchronization. Song *et al.* [45], [46] studied a class of uncertain fractional-order nonlinear systems subject to uncertainties and external disturbances and the adaptive output feedback resilient control problem, and designed a fractional adaptive backstepping neuro-fuzzy sliding mode controller with neuro-fuzzy network system and the fractional Lyapunov stability theory and the finite-time stability theory, and pointed out that observer-based adaptive output feedback control scheme for fractional-order (FO) nonlinear systems is one of our future work. Today, most three-dimensional fractional-order chaotic systems require three control laws for synchronous control [47], [48], and how to design fewer control laws needs further study, and how to optimize the control law that makes it contain only state variables is also a question worth studying.

Because of the advantages of entropy in complexity analysis, this paper combines the complexity analysis of fractional chaotic system with entropy. Firstly, for the integer-order Jafari-Sprott chaotic system, the classical Lyapunov exponent, Poincaré section, and bifurcation diagram are used to analyze dynamics. Secondly, the fractional-order Jafari-Sprott chaotic system is taken as an example to introduce the decomposition steps of the Adomian decomposition method in detail. Then, the effects of system parameters and orders on the complexity of fractional-order Jafari-Sprott chaotic system based on Adomian decomposition method and three entropy are analyzed. The combination of entropy and the complexity of fractional-order chaotic system can better reflect the characteristics of the system. Finally, synchronization control of the fractional-order Jafari-Sprott chaotic system is accomplished by sliding mode control and the frequency distribution model of the fractional-order integral operator respectively.

II. DYNAMICS ANALYSIS OF INTEGER-ORDER JAFARI-SPROTT CHAOTIC

A. INTRODUCTION TO MATHEMATICAL MODEL

The mathematical model of the integer-order Jafari-Sprott chaotic system [49] is as following:

$$\begin{cases} \dfrac{dx}{dt} = y \\ \dfrac{dy}{dt} = -x + yz \\ \dfrac{dz}{dt} = -x - axy - bxz \end{cases} \tag{1}$$

In this three-dimensional system, x, y and z are system variables, a and b are system parameters. When $a = 15$, $b = 1$ and the initial values is (0, 0.5, 0.5), the system is in a chaotic state. By using the Runge-Kutta method, phase space diagram is shown in Figure 1.

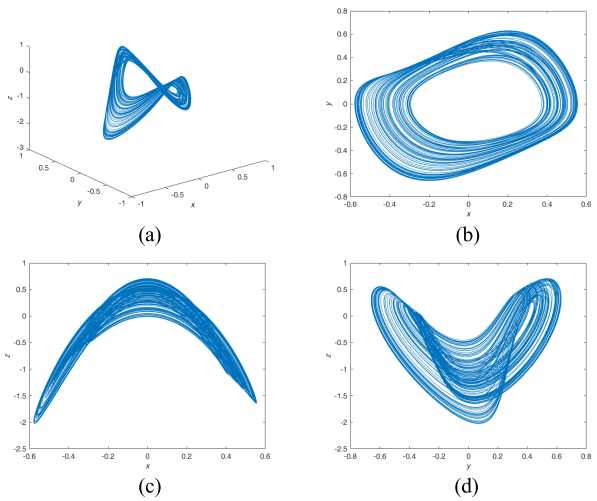

FIGURE 1. Phase space diagram of each plan.

Time domain waveform of each variable is shown in Figure 2.

B. B ANALYSIS OF DYNAMIC CHARACTERISTICS

1) LYAPUNOV EXPONENT

Lyapunov exponent is a quantitative criterion for describing the state evolution of dynamical systems, and used to measure the degree of attraction or separation of two adjacent trajectories with different initial conditions in phase space according to the exponential law over time. This ratio of trajectory

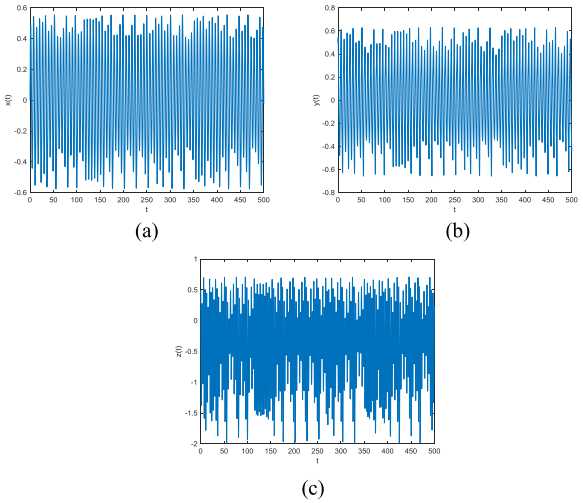

FIGURE 2. Time domain waveform of each variable.

convergence or divergence is called the Lyapunov exponent. In a three-dimensional chaotic system, there is a Lyapunov exponent greater than 0, which means that the system is in a chaotic state.

For integer-order Jafari-Sprott chaotic system, when the system parameters $a = 15$, $b = 1$ and the initial values is $(0, 0.5, 0.5)$, the Lyapunov exponent diagram is shown in Figure 3. Fixed system parameter $b = 1$ and the system parameter $a \in [10, 20]$, its Lyapunov exponent is shown in Figure 4.

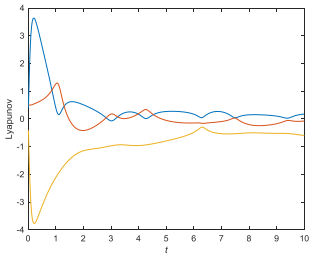

FIGURE 3. Lyapunov exponent diagram.

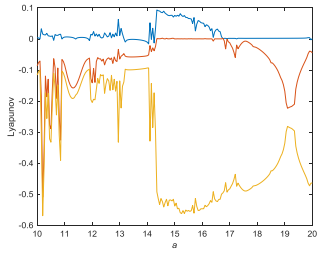

FIGURE 4. Lyapunov exponent diagram with $a \in [10, 20]$.

2) POINCARÉ SECTION

A section is selected in the multi-dimensional phase space. This section is not tangent to the trajectory, and convenient for observing the motion characteristics and changes of the system. This section is called the Poincaré section. When the system parameters $a = 15, b = 1, h = 0.001$, h is the step length and the initial values is $(0, 0.5, 0.5)$, the Poincaré section of the integer-order Jafari-Sprott chaotic system is shown in Figure 5. Figure 5 shows that the Poincaré section is a dense cluster of slices, so it can be concluded that the Jafari-Sprott chaotic system is in a chaotic state.

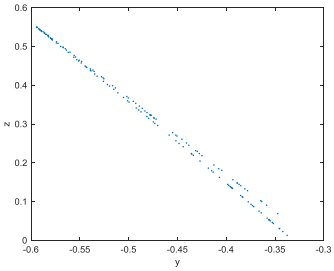

FIGURE 5. Poincaré section diagram.

3) BIFURCATION DIAGRAM

Bifurcation refers to the type of dynamic movement changed when a parameter changes. When the system parameters $a \in [10, 20]$, the bifurcation diagram of the Jafari-Sprott chaotic system is shown in Figure 6. It can be seen from Figure 6 with the change of the system parameter a, the system continuously branches between different states, and finally the system reaches a chaotic state.

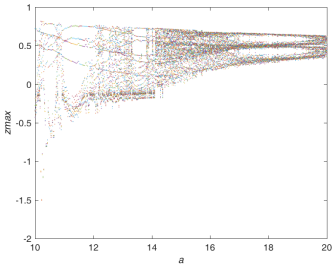

FIGURE 6. Bifurcation diagram.

III. NUMERICAL ANALYSIS OF FRACTIONAL-ORDER JAFARI-SPROTT CHAOTIC SYSTEM BASED ON ADOMIAN METHOD

A. COMMON DEFINITION OF FRACTIONAL CALCULUS

1) The Grünwald-Letnikov fractional differential is defined as following [50]:

$$ {}_aD_t^q f(t) = \frac{d^q f(t)}{d(t-a)^q} = \lim_{N\to\infty} [\frac{t-a}{N}]^{-q} \times \sum_{j=0}^{N-1} (-1)^j \binom{q}{j} f(t - j[\frac{t-a}{N}]) \quad (2) $$

where, ${}_aD_t^q$ is the fractional calculus operator. ${}_aD_t^q$ can simultaneously represent the derivative of the fractional order and

the integral of the fractional order. When $q > 0$, ${}_aD_t^q$ represents the derivative. When $q < 0$, ${}_aD_t^q$ represents the integral.

2) The Riemann-Liouville fractional differential is defined as following [51]:

$$ {}_aD_t^q f(t) \begin{cases} \dfrac{1}{\Gamma(-q)} \displaystyle\int_a^t (t-\tau)^{-q-1} f(\tau) d\tau & q < 0 \\ f(t) & q = 0 \\ D^n[{}_aD_t^{q-n} f(t)] & q > 0 \end{cases} \tag{3} $$

The power series and constant of q-order differential are defined respectively as following:

$$ D_{t_0}^q t^r = \frac{\Gamma(r+1)}{\Gamma(r+1-q)} (t-t_0)^{r-q} \tag{4} $$

$$ D_{t_0}^q C = \frac{C}{\Gamma(1-q)} (t-t_0)^{-q} \tag{5} $$

where $\Gamma(\cdot)$ is the Gamma function. This is the most basic function in fractional calculus, which is defined as:

$$ \Gamma(x) = \int_0^\infty t^{x-1} e^{-t} dt \tag{6} $$

When $x \in [-5, 5]$, the Gamma function is shown in Figure 7. Places marked in Figure 7 are 0!, 1!, 2!, 3!.

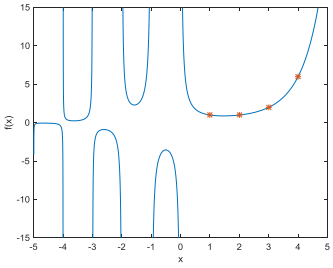

FIGURE 7. Gamma function graph.

3) The Caputo fractional differential is defined as following [52]:

$$ {}_aD_{t_0}^q f(t) = \begin{cases} \dfrac{1}{\Gamma(m-q)} \displaystyle\int_0^t \frac{f(m)(\tau) d\tau}{(t-\tau)^{q+1-m}} \\ \qquad m-1 < q < m \\ \dfrac{d^m}{dt^m} f(t) \\ \qquad q = m \end{cases} \tag{7} $$

The q-order differential of constant and power function is defined respectively as following:

$$ D_{t_0}^q t^r = \frac{\Gamma(r+1)}{\Gamma(r+1-q)} (t-t_0)^{r-q} \tag{8} $$

$$ D_{t_0}^q C = 0 \tag{9} $$

B. THE ADOMIAN DECOMPOSITION METHOD

The Adomian decomposition method [53] is the latest proposed time-domain approximation algorithm, and suitable for numerical solution of fractional-order chaotic system. This algorithm does not require discrimination and takes up a lot of computer memory, and can provide high-precision, fast-convergent numerical analysis.

For fractional-order chaotic system

$$ D_{t_0}^q x(t) = f(x(t)) + g(t) \tag{10} $$

where, $x(t) = [x_1(t), x_2(t), \ldots, x_n(t)]^T$ is the corresponding function variable, $g(t) = [g_1(t), g_2(t), \ldots, g_n(t)]^T$ is constant. The system is divided into three parts as following:

$$ \begin{cases} D_{t_0}^q x(t) = Lx(t) + Nx(t) + g(t) \\ x(k)(t_0^+) = b_k, & k = 0, \ldots, m-1 \\ m \in N, & m - m < q \le m \end{cases} \tag{11} $$

The nonlinear term is decomposed according to the following formula:

$$ \begin{cases} A_j^i = \dfrac{1}{i!} [\dfrac{d^i}{d\lambda^i} N(v_j^i(\lambda))]_{\lambda=0} \\ v_j^i = \displaystyle\sum_{k=0}^{i} (\lambda)^k x_j^k \end{cases} \tag{12} $$

where the nonlinear term can be expressed as following:

$$ Nx = \sum_{i=0}^{\infty} A^i(x^0, x^1, x^2, \ldots, x^i) \tag{13} $$

The solution of the equation is as following:

$$ x = \sum_{i=0}^{\infty} x^i = J_{t_0}^q L \sum_{i=0}^{\infty} x^i + J_{t_0}^q \sum_{i=0}^{\infty} A^i + J_{t_0}^q g + \Phi \tag{14} $$

where $\Phi = \sum_{k=0}^{m-1} b_k \frac{(t-t_0)^k}{k!}$ is the initial condition to satisfy the system, and its iterative relationship is as following:

$$ \begin{cases} x^0 = J_{t_0}^q g + \Phi \\ x^1 = J_{t_0}^q L x^0 + J_{t_0}^q A^0(x^0) \\ x^2 = J_{t_0}^q L x^1 + J_{t_0}^q A^1(x^0, x^1) \\ \ldots \\ x^i = J_{t_0}^q L x^{i-1} + J_{t_0}^q A^{i-1}(x^0, x^1, \ldots, x^{i-1}) \\ \ldots \end{cases} \tag{15} $$

The mathematical model of the fractional-order Jafari-Sprott chaotic system is as following:

$$ \begin{cases} D_{t_0}^q x_1 = x_2 \\ D_{t_0}^q x_2 = -x_1 + x_2 x_3 \\ D_{t_0}^q x_3 = -x_1 - a x_1 x_2 - b x_1 x_3 \end{cases} \tag{16} $$

The linear and nonlinear terms in this system respectively are as following:

$$\begin{bmatrix} Lx_1 \\ Lx_2 \\ Lx_3 \end{bmatrix} = \begin{bmatrix} x_2 \\ -x_1 \\ -x_1 \end{bmatrix}, \quad \begin{bmatrix} Nx_1 \\ Nx_2 \\ Nx_3 \end{bmatrix} = \begin{bmatrix} 0 \\ x_2x_3 \\ -ax_1x_2 - bx_1x_3 \end{bmatrix} \tag{17}$$

Decompose the nonlinear term according to Equation (12). The decomposition Nx_2 process is as following:

$$\begin{aligned} A_2^0 &= x_2^0x_3^0 \\ A_2^1 &= [(\lambda^k x_2^k)(\lambda^k x_3^k)]' \\ &= [(\mathrm{k}\lambda^{k-1}\mathrm{x}_2^k)(\lambda^k \mathrm{x}_3^k) + (\mathrm{k}\lambda^{k-1}\mathrm{x}_3^k)(\lambda^k \mathrm{x}_2^k)] \\ &= \mathrm{x}_2^1\mathrm{x}_3^0 + x_2^0x_3^1 \\ A_2^2 &= \frac{1}{2!}[(k\lambda^{k-1}x_2^k)(\lambda^k x_3^k) + (k\lambda^{k-1}x_3^k)(\lambda^k x_2^k)]' \\ &= \frac{1}{2!}[2x_2^2x_3^0 + 2x_2^1x_3^1 + 2x_2^0x_3^2] \\ &= x_2^2x_3^0 + x_2^1x_3^1 + x_2^0x_3^2 \\ A_2^3 &= \frac{1}{3!}[(k(k-1)\lambda^{k-2}x_2^k)(\lambda^k x_3^k) + 2(k\lambda^{k-1}x_2^k)(k\lambda^{k-1}x_3^k) \\ &\quad + (\lambda^k x_2^k)(k(k-1)\lambda^{k-2}x_3^k)]' \\ &= \frac{1}{3!}[6x_2^3x_3^0 + 6x_2^2x_3^1 + 6x_2^1x_3^2 + 6x_2^0x_3^3] \\ &= x_2^3x_3^0 + x_2^2x_3^1 + x_2^1x_3^2 + x_2^0x_3^3 \end{aligned} \tag{18}$$

Since each decomposition principle is the same, Equation (18) only lists the specific decomposition process of the previous three terms. The complete decomposition result is as following:

$$\begin{cases} A_2^0 = x_2^0x_3^0 \\ A_2^1 = x_2^1x_3^0 + x_2^0x_3^1 \\ A_2^2 = x_2^2x_3^0 + x_2^1x_3^1 + x_2^0x_3^2 \\ A_2^3 = x_2^3x_3^0 + x_2^2x_3^1 + x_2^1x_3^2 + x_2^0x_3^3 \\ A_2^4 = x_2^4x_3^0 + x_2^3x_3^1 + x_2^2x_3^2 + x_2^1x_3^3 + x_2^0x_3^4 \\ A_2^5 = x_2^5x_3^0 + x_2^4x_3^1 + x_2^3x_3^2 + x_2^2x_3^3 + x_2^1x_3^4 + x_2^0x_3^5 \end{cases} \tag{19}$$

$$\begin{cases} A_3^0 = a(-x_1^0x_2^0) - bx_1^0x_3^0 \\ A_3^1 = a(-x_1^1x_2^0 - x_1^0x_2^1) - b(x_1^1x_3^0 + x_1^0x_3^1) \\ A_3^2 = a(-x_1^2x_2^0 - x_1^1x_2^1 - x_1^0x_2^2) \\ -b(x_1^2x_3^0 + x_1^1x_3^1 + x_1^0x_3^2) \\ A_3^3 = a(-x_1^3x_2^0 - x_1^2x_2^1 - x_1^1x_2^2 - x_1^0x_2^3) \\ -b(x_1^3x_3^0 + x_1^2x_3^1 + x_1^1x_3^2 + x_1^0x_3^3) \\ A_3^4 = a(-x_1^4x_2^0 - x_1^3x_2^1 - x_1^2x_2^2 - x_1^1x_2^3 - x_1^0x_2^4) \\ -b(x_1^4x_3^0 + x_1^3x_3^1 + x_1^2x_3^2 + x_1^1x_3^3 + x_1^0x_3^4) \\ A_3^5 = a(-x_1^5x_2^0 - x_1^4x_2^1 - x_1^3x_2^2 - x_1^2x_2^3 - x_1^1x_2^4 - x_1^0x_2^5) \\ -b(x_1^5x_3^0 + x_1^4x_3^1 + x_1^3x_3^2 + x_1^2x_3^3 + x_1^1x_3^4 + x_1^0x_3^5) \end{cases} \tag{20}$$

The initial condition is as following:

$$\begin{cases} x_1^0 = x_1(t_0) \\ x_2^0 = x_2(t_0) \\ x_3^0 = x_3(t_0) \end{cases} \tag{21}$$

Let $c_1^0 = x_1^0, c_2^0 = \mathrm{x}_2^0, c_3^0 = \mathrm{x}_3^0$, we can obtain from Equation (15):

$$Lx^0 = \begin{Bmatrix} x_2^0 \\ -x_1^0 \\ -x_1^0 \end{Bmatrix} = \begin{Bmatrix} c_2^0 \\ -c_1^0 \\ -c_1^0 \end{Bmatrix} \tag{22}$$

$$J_{t_0}^q Lx^0 = \begin{Bmatrix} x_2^0 \\ -x_1^0 \\ -x_1^0 \end{Bmatrix} \frac{(t-t_0)^q}{\Gamma(q+1)} \tag{23}$$

$$\begin{aligned} A^0x^0 &= \begin{Bmatrix} A_1^0(x^0) \\ A_2^0(x^0) \\ A_3^0(x^0) \end{Bmatrix} = \begin{Bmatrix} 0 \\ x_2^0x_3^0 \\ -ax_1^0x_2^0 - bx_1^0x_3^0 \end{Bmatrix} \\ &= \begin{Bmatrix} 0 \\ c_2^0c_3^0 \\ -ac_1^0c_2^0 - bc_1^0c_3^0 \end{Bmatrix} \end{aligned} \tag{24}$$

$$J_{t_0}^q A^0(x^0) = \begin{Bmatrix} 0 \\ c_2^0c_3^0 \\ -ac_1^0c_2^0 - bc_1^0c_3^0 \end{Bmatrix} \frac{(t-t_0)^q}{\Gamma(q+1)} \tag{25}$$

$$\begin{aligned} x^1 &= J_{t_0}^q Lx^0 + J_{t_0}^q A^0(x^0) = \begin{Bmatrix} c_2^0 \\ -c_1^0 \\ -c_1^0 \end{Bmatrix} \frac{(t-t_0)^q}{\Gamma(q+1)} \\ &\quad + \begin{Bmatrix} 0 \\ c_2^0c_3^0 \\ -ac_1^0c_2^0 - bc_1^0c_3^0 \end{Bmatrix} \frac{(t-t_0)^q}{\Gamma(q+1)} \\ &= \begin{Bmatrix} \mathrm{c}_2^2 \\ -c_1^0 + c_2^0c_3^0 \\ -c_1^0 - ac_1^0c_2^0 - bc_1^0c_3^0 \end{Bmatrix} \frac{(t-t_0)^q}{\Gamma(q+1)} \end{aligned} \tag{26}$$

$$\begin{cases} x_1^1 = c_2^0 \dfrac{(t-t_0)^q}{\Gamma(q+1)} \\ x_2^1 = [-c_1^0 + c_2^0c_3^0] \dfrac{(t-t_0)^q}{\Gamma(q+1)} \\ x_3^1 = [-c_1^0 - ac_1^0c_2^0 - bc_1^0c_3^0] \dfrac{(t-t_0)^q}{\Gamma(q+1)} \end{cases} \tag{27}$$

Assign the coefficient to the corresponding variable, we can get:

$$\begin{cases} c_1^1 = c_2^0 \\ c_2^1 = [-c_1^0 + c_2^0c_3^0] \\ c_3^1 = [-c_1^0 - ac_1^0c_2^0 - bc_1^0c_3^0] \end{cases} \tag{28}$$

The derivation method for the remaining 5 items is the same as the above formula:

$$\begin{cases} c_1^2 = c_2^1 \\ c_2^2 = [-c_1^1 + c_2^1c_3^0 + c_2^0c_3^1] \\ c_3^2 = [-c_1^1 + a(-c_1^1c_2^0 - c_1^0c_2^1) \\ +b(-c_1^1c_3^0 - c_1^0c_3^1)] \end{cases} \tag{29}$$

$$\begin{cases} c_1^3 = c_2^2 \\ c_2^3 = [-c_1^2 + c_2^2c_3^0 + c_2^1c_3^1 \dfrac{\Gamma(2q+1)}{\Gamma(q+1)^2} + c_2^0c_3^2] \\ c_3^3 = [-c_1^2 + a(-c_1^2c_2^0 - c_1^1c_2^1 \dfrac{\Gamma(2q+1)}{\Gamma(q+1)^2} - c_1^0c_2^2) \\ +b(-c_1^2c_3^0 - c_1^1c_3^1 \dfrac{\Gamma(2q+1)}{\Gamma(q+1)^2}) - c_1^0c_3^2] \end{cases} \tag{30}$$

$$\begin{cases} c_1^4 = c_2^3 \\ c_2^4 = [-c_1^3 + c_2^3 c_3^0 + c_2^2 c_3^1 + c_2^1 c_3^2 \dfrac{\Gamma(3q+1)}{\Gamma(q+1)\Gamma(2q+1)} \\ + c_2^0 c_3^3] \\ c_3^4 = [-c_1^3 + a(-c_1^3 c_2^0 - c_1^2 c_2^1 + c_1^1 c_2^2 \\ \dfrac{\Gamma(3q+1)}{\Gamma(q+1)\Gamma(2q+1)} \\ - c_1^0 c_2^3) \\ + b(-c_1^3 c_3^0 - c_1^2 c_3^1 + c_1^1 c_3^2 \dfrac{\Gamma(3q+1)}{\Gamma(q+1)\Gamma(2q+1)}) \\ - c_1^0 c_3^3] \end{cases} \tag{31}$$

$$\begin{cases} c_1^5 = c_2^4 \\ c_2^5 = [-c_1^4 + c_2^4 c_3^0 + (c_2^3 c_3^1 + c_2^1 c_3^3) \dfrac{\Gamma(4q+1)}{\Gamma(q+1)\Gamma(3q+1)} \\ + c_2^2 c_3^2 \dfrac{\Gamma(4q+1)}{\Gamma(2q+1)^2} + c_2^0 c_3^4] \\ c_3^5 = [-c_1^4 + a(-c_1^4 c_2^0 - (c_1^3 c_2^1 + c_1^1 c_2^3) \\ \dfrac{\Gamma(4q+1)}{\Gamma(q+1)\Gamma(3q+1)} - c_1^2 c_2^2 \dfrac{\Gamma(4q+1)}{\Gamma(2q+1)^2} - c_1^0 c_2^4) \\ + b(-c_1^4 c_3^0 - (c_1^3 c_3^1 + c_1^1 c_3^3) \dfrac{\Gamma(4q+1)}{\Gamma(q+1)\Gamma(3q+1)}) \\ - c_1^2 c_3^2 \dfrac{\Gamma(4q+1)}{\Gamma(2q+1)^2} - c_1^0 c_3^4] \end{cases} \tag{32}$$

$$\begin{cases} c_1^6 = c_2^5 \\ c_2^6 = [-c_1^5 + c_2^5 c_3^0 + (c_2^4 c_3^1 + c_2^1 c_3^4) \dfrac{\Gamma(5q+1)}{\Gamma(q+1)\Gamma(4q+1)} \\ + (c_2^3 c_3^2 + c_2^2 c_3^3) \dfrac{\Gamma(5q+1)}{\Gamma(2q+1)\Gamma(3q+1)} + c_2^0 c_3^5] \\ c_3^6 = [-c_1^5 + a(-c_1^5 c_2^0 - (c_1^4 c_2^1 + c_1^1 c_2^4) \\ \dfrac{\Gamma(5q+1)}{\Gamma(q+1)\Gamma(4q+1)} - (c_1^3 c_2^2 + c_1^2 c_2^3) \\ \dfrac{\Gamma(5q+1)}{\Gamma(2q+1)\Gamma(3q+1)} - c_1^0 c_2^5) \\ + b(-c_1^5 c_3^0 - (c_1^4 c_3^1 + c_1^1 c_3^4) \dfrac{\Gamma(5q+1)}{\Gamma(q+1)\Gamma(4q+1)}) \\ - (c_1^3 c_3^2 + {}_1^2 c_3^3) \dfrac{\Gamma(5q+1)}{\Gamma(2q+1)\Gamma(3q+1)} - c_1^0 c_3^5] \end{cases} \tag{33}$$

At this time, the solution of the system equation can be expressed as:

$$x_j(t) = c_j^0 + c_j^1 \frac{(t-t_0)^q}{\Gamma(q+1)} + c_j^2 \frac{(t-t_0)^{2q}}{\Gamma(2q+1)} + c_j^3 \frac{(t-t_0)^{3q}}{\Gamma(3q+1)} + c_j^4 \frac{(t-t_0)^{4q}}{\Gamma(4q+1)} + c_j^5 \frac{(t-t_0)^{5q}}{\Gamma(5q+1)} + c_j^6 \frac{(t-t_0)^{6q}}{\Gamma(6q+1)} \tag{34}$$

When $a = 15$, $b = 1$, $q = 0.96$, and the initial values is $(0, 0.5, 0.5)$, phase space diagram is shown in Figure 8.

The Adomian decomposition method has the advantages of high precision, no occupy computer memory, no need of discretization, etc. It is suitable for cases where the maximum number of nonlinear terms is less than 3. If the highest order of nonlinear terms is greater than or equal to 3, then the calculation amount of its decomposition process is large, and the Adomian decomposition method is not recommended.

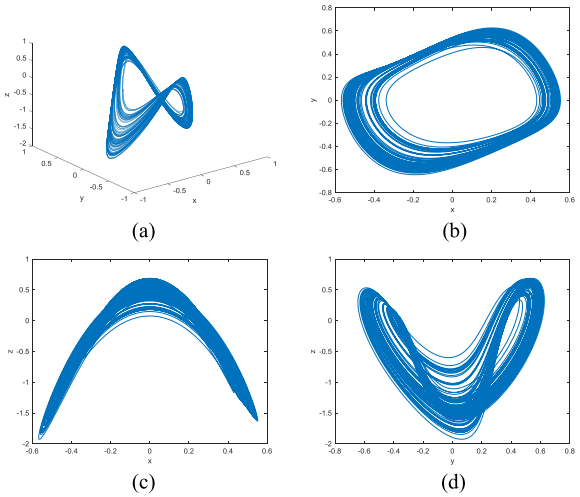

FIGURE 8. Phase space diagram of each plane.

IV. COMPLEXITY ANALYSIS OF FRACTIONAL-ORDER JAFARI-SPROTT CHAOTIC SYSTEM

The complexity of chaotic characteristics is also a method for analyzing the dynamic characteristics of chaotic system. It has the same effect as the Lyapunov exponent, Poincaré section, and bifurcation diagram. In a nutshell, complexity is the degree to which a correlation algorithm is used to calculate the approximate random sequence. The greater the complexity, the closer the random sequence is, the higher the security is. The complexity of chaotic sequences is divided into behavioral complexity and structural complexity. Behavioral complexity refers to using a certain method to measure the probability of a sequence generating a new pattern in a short time window from the chaotic sequence itself. The larger the probability of generating a new pattern, the more complex the sequence is. Structural complexity refers to analyzing the complexity of a sequence by changing frequency characteristics, energy spectrum characteristics, etc. The more balanced the energy spectrum distribution of the sequence, the more complex the sequence is.

A. FUZZY ENTROPY ALGORITHM

For judging the complexity of a sequence, fuzzy entropy is an effective measurement algorithm, and it has lower sensitivity dependence on sequence length, phase space dimension, and similarity tolerance. The algorithm process [54] is as following:

Step 1: Perform phase space reconstruction of the sequence. For a given sequence $[u(1), u(2), \ldots, u(N)]$, the reconstructed phase space is:

$$X(i) = [u(i), u(i+1), \ldots, u(i+1-m)] - u_0(i) \tag{35}$$

where, $u_0(i) = \frac{1}{m} \sum_{j=0}^{m-1} u(i+j)$.

Step 2: Introduce fuzzy membership function. The fuzzy membership function is defined as:

$$A(x) = \begin{cases} 1, & x = 0 \\ \exp[-\ln\ (2)(\frac{x}{r})^2], & x > 0 \end{cases} \tag{36}$$

where, r is the similar tolerance. The fuzzy membership function is given:

$$A_{ij}^m = \exp[-\ln\ (2)(\frac{d_{ij}^m}{r})^2], \quad j = 1, 2, \ldots,\ N - m + 1,\ j \neq i \tag{37}$$

where,

$$\begin{aligned} d_{ij}^m &= d[X(i), X(j)] \\ &= \max_{p=1,2,\ldots,m}(|u(i+p-1) - u_0(i)| \\ &\quad - |u(j+p-1) - u_0(j)|) \end{aligned} \tag{38}$$

is the maximum absolute distance between the vectors $X(i), X(j)$.

Step 3: Calculate the fuzzy entropy. Average value each i to get:

$$C_i^m(r) = \frac{1}{N-m} \sum_{j=1, j\neq i}^{N-m+1} A_{ij}^m \tag{39}$$

$$\Phi^m(r) = \frac{1}{N-m+1} \sum_{i=1}^{N-m+1} C_i^m(r) \tag{40}$$

So the fuzzy entropy is:

$$Fuzzy(m, r, N) = \ln \Phi^m(r) - \ln \Phi^{m+1}(r) \tag{41}$$

where, m, r, N are the dimensions of phase space, similarity tolerance, and number of selected data, select $m = 2$, $r = 0.2 * SD$, $N = 15000$, SD is the standard deviation of N. When the system parameters $b = 1$, $q = 0.96$, $a \in [12, 20]$, the fuzzy entropy complexity of the fractional-order Jafari-Sprott chaotic system is shown in Figure 9 (a). When the system parameters $a = 15, b = 1, q \in [0.2, 1]$, the fuzzy entropy complexity of the fractional-order Jafari-Sprott chaotic system is shown in Figure 9 (b). When the system parameters $a = 15$, $q = 0.96, b \in [0.2, 1.2]$, the fuzzy entropy complexity of the fractional-order Jafari-Sprott chaotic system is shown in Figure 9 (c).

A single parameter change is not as complicated as a multi-parameter change. In the following, the chromatogram is used to simulate and analyze the situation under the changes of the two parameters. When $a \in [12, 20], q \in [0.2, 1]$, the chromatogram of the change of fuzzy entropy complexity is shown in Figure 10 (a). When $b \in [0.2, 1.2], q \in [0.2, 1]$, the chromatogram of the change of fuzzy entropy complexity is shown in Figure 10 (b). When $a \in [12, 20], b \in [0.2, 1.2]$, the chromatogram of the change of fuzzy entropy complexity is shown in Figure 10 (c).

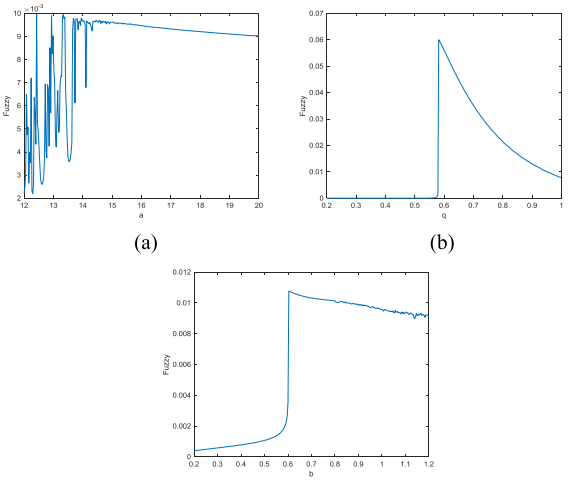

FIGURE 9. Fuzzy entropy complexity.

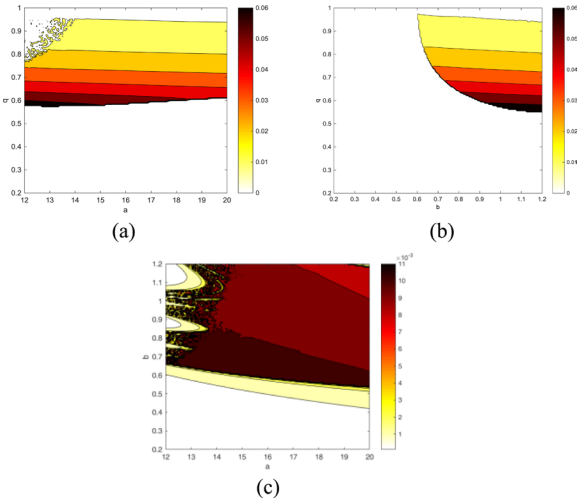

FIGURE 10. Fuzzy entropy complexity chromatogram.

B. SAMPLE ENTROPY ALGORITHM

Sample entropy is a method for measuring the complexity of a sequence, and it is used in a variety of research fields, especially medical biology. The algorithmic process [55] is as following:

Step 1: Perform phase space reconstruction of the sequence. For a given sequence $[x(1), x(2), \ldots, x(N)]$, the reconstructed phase space is:

$$\begin{cases} X_m(1) = \{x_1, x_2, \ldots, x_m\} - \overline{X_1^m} \\ X_m(2) = \{x_2, x_3, \ldots, x_{m+1}\} - \overline{X_2^m} \\ \ldots \\ X_m(i) = \{x_i, x_{i+1}, \ldots, x_{i+m}\} - \overline{X_i^{m+1}} \\ \ldots \\ X_m(N-m) = \{x_{N-m}, x_{N-m+1}, \ldots, x_{N-1}\} - \overline{X_{N-m}^m} \end{cases} \tag{42}$$

$$\begin{cases} X_{m+1}(1) = \{x_1, x_2, \ldots, x_{m+1}\} - \overline{X_1^{m+1}} \\ X_{m+1}(2) = \{x_2, x_3, \ldots, x_{m+2}\} - \overline{X_2^{m+1}} \\ \cdots \\ X_{m+1}(i) = \{x_i, x_{i+1}, \ldots, x_{i+m}\} - \overline{X_i^{m+1}} \\ \cdots \\ X_{m+1}(N-m) = \{x_{N-m}, x_{N-m+1}, \ldots, x_N\} - \overline{X_{N-m}^{m+1}} \end{cases} \tag{43}$$

where, $\overline{X_i^m}$, $\overline{X_i^{m+1}}$ is the mean of the sequences $\{x_i, x_{i+1}, \ldots, x_{i+m-1}\}$ and $\{x_i, x_{i+1}, \ldots, x_{i+m}\}$ respectively.

Step 2: Calculate the distance between the vectors. The distance between the vectors $X_m(i)$, $X_m(j)$ is defined as d, then the distance between the two vectors can be defined as:

$$\begin{cases} d[X_m(i), X_m(j)] = \max |x(i+k) - x(j+k)| \\ d[X_{m+1}(i), X_{m+1}(j)] = \max |x(i+k) - x(j+k)| \end{cases} \tag{44}$$

Step 3: Calculate the sample entropy. Given a similar capacity r, count the number that the distance between the vectors is less than the similarity capacity, and calculate the ratio to the total number $A_r^m(i)$ and $A_r^{m+1}(i)$. It is specifically defined as:

$$\begin{cases} A_r^m(i) = \dfrac{d[X_m(i), X_m(j)] \le r}{N-m-1} \\ A_r^{m+1}(i) = \dfrac{d[X_{m+1}(i), X_{m+1}(j)] \le r}{N-m-1} \end{cases} \tag{45}$$

The average of the reconstructed m-dimensional and $m+1$-dimensional sequences is recorded as $B^m(r)$ and $B^{m+1}(r)$, and the specifically defined is as following:

$$\begin{cases} B^m(r) = \dfrac{1}{N-m} \displaystyle\sum_{i=1}^{N-m} A_r^m(i) \\ B^{m+1}(r) = \dfrac{1}{N-m} \displaystyle\sum_{i=1}^{N-m} A_r^{m+1}(i) \end{cases} \tag{46}$$

The sample entropy calculation formula is:

$$Samp(m, r, N) = -\ln \frac{B^{m+1}(r)}{B^m(r)} \tag{47}$$

where, m, r, N are the dimensions of phase space, similarity tolerance, and number of selected data, select $m = 2$, $r = 0.2 * SD$, $N = 15000$, SD is the standard deviation of N. When the system parameters $b = 1$, $q = 0.96$, $a \in [12, 20]$, the sample entropy complexity of the fractional-order Jafari-Sprott chaotic system is shown in Figure 11 (a). When the system parameters $a = 15$, $b = 1$, $q \in [0.2, 1]$, the sample entropy complexity of the fractional-order Jafari-Sprott chaotic system is shown in Figure 11 (b). When the system parameters $a = 15$, $q = 0.96$, $b \in [0.2, 1.2]$, the sample entropy complexity of the fractional-order Jafari-Sprott chaotic system is shown in Figure 11 (c).

When $a \in [12, 20]$, $q \in [0.2, 1]$, the chromatogram of the change of sample entropy complexity is shown in Figure 12 (a). When $b \in [0.2, 1.2]$, $q \in [0.2, 1]$, the chromatogram of the change of sample entropy complexity is shown in Figure 12 (b). When $a \in [12, 20]$, $b \in [0.2, 1.2]$, the chromatogram of the change of sample entropy complexity is shown in Figure 12 (c).

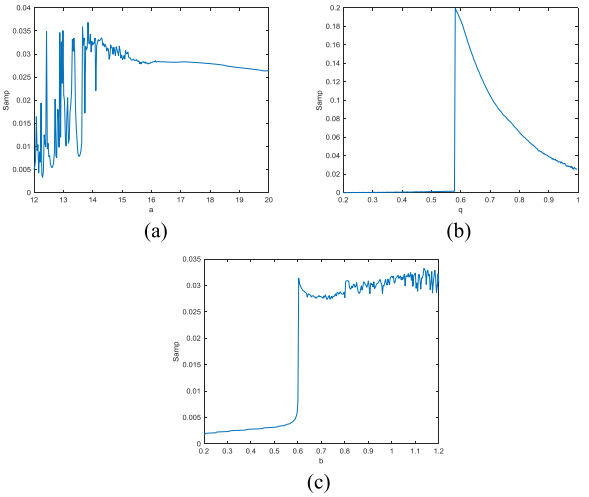

FIGURE 11. Sample entropy complexity.

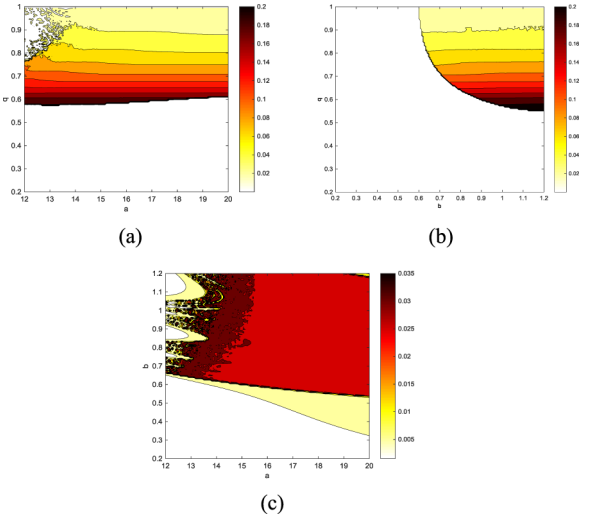

FIGURE 12. Sample entropy chromatogram.

C. DISPERSION ENTROPY ALGORITHM

The dispersion entropy algorithm process [56] is as following:

Step 1: Map the sequence $x_j (j = 1, 2, \ldots, N)$ to $y = \{y_j, j = 1, 2, \ldots, N\}$ by using a normal distribution, and then use a linear transformation to map y to the range of $[1, 2, \cdots, c]$

$$z_j^c = round\left(cy_j + 0.5\right) \tag{48}$$

where *round* and c respectively represent integer function and the number of categories.

Step 2: Calculate the embedded vector $z_i^{m,c}$

$$z_i^{m,c} = \left\{z_i^c, z_{i+d}^c, \ldots, z_{i+(m-1)d}^c\right\} \tag{49}$$

where $i = 1, 2, \ldots, N-(m-1)d$, m and d respectively represent embedding dimension and time delay.

Step 3: Create an embedding vector c with an embedding dimension m and a time delay d. Each time series c is mapped to a decentralized pattern c, where $x, y = \{y_1, y_2, \cdots, y_N\}$.

Step 4: Calculate the probability $p\left(\pi_{v_0,v_1,\ldots,v_{m-1}}\right)$ for each dispersion pattern $\pi_{v_0,v_1,\ldots,v_{m-1}}$:

$$p\left(\pi_{v_0,v_1,\ldots,v_{m-1}}\right) = \frac{N_b\left(\pi_{v_0,v_1,\ldots,v_{m-1}}\right)}{N-(m-1)d} \tag{50}$$

where $N_b\left(\pi_{v_0,v_1,\ldots,v_{m-1}}\right)$ represents the number of $z_i^{m,c}$ mapped to $\pi_{v_0,v_1,\ldots,v_{m-1}}$. So $p\left(\pi_{v_0,v_1,\ldots,v_{m-1}}\right)$ can be expressed as the ratio of the number of $z_i^{m,c}$ mapped to $\pi_{v_0,v_1,\ldots,v_{m-1}}$ to the number of elements in $z_i^{m,c}$.

Step 5: According to the definition of Shannon, the dispersion entropy of original time series is defined as:

$$DE(x,m,c,d) = -\sum_{\pi=1}^{c^m} p\left(\pi_{v_0,v_1,\ldots,v_{m-1}}\right) \times \ln\left(p\left(\pi_{v_0,v_1,\ldots,v_{m-1}}\right)\right) \tag{51}$$

where x is the number of selected data, m is the embedding dimension, c is the category, and d is the time delay, select $x = 15000$, $m = 2$, $c = 3$, $d = 1$. When the system parameters $b = 1$, $q = 0.96$, $a \in [12, 20]$, the dispersion entropy complexity of the fractional-order Jafari-Sprott chaotic system is shown in Figure 13 (a). When the system parameters $a = 15$, $b = 1$, $q \in [0.2, 1]$, the dispersion entropy complexity of the fractional-order Jafari-Sprott chaotic system is shown in Figure 13 (b). When the system parameters $a = 15$, $q = 0.96$, $b \in [0.2, 1.2]$, the dispersion entropy complexity of the fractional-order Jafari-Sprott chaotic system is shown in Figure 13 (c).

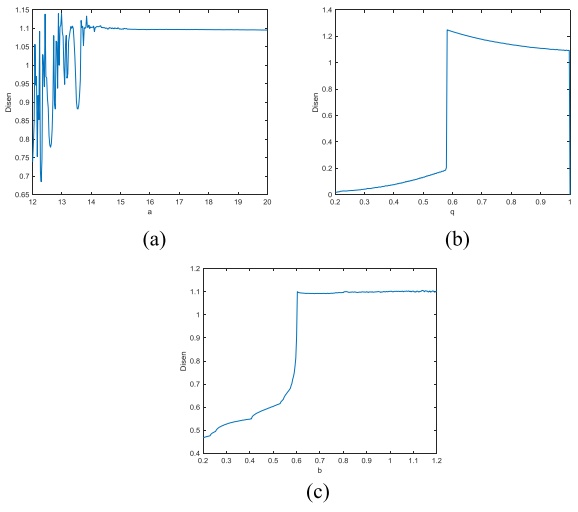

FIGURE 13. Dispersion entropy complexity.

When $a \in [12, 20]$, $q \in [0.2, 1]$, the chromatogram of the change of dispersion entropy complexity is shown in Figure 14 (a). When $b \in [0.2, 1.2]$, $q \in [0.2, 1]$, the chromatogram of the change of dispersion entropy complexity is shown in Figure 14 (b). When $a \in [12, 20]$, $b \in [0.2, 1.2]$, the chromatogram of the change of dispersion entropy complexity is shown in Figure 14 (c).

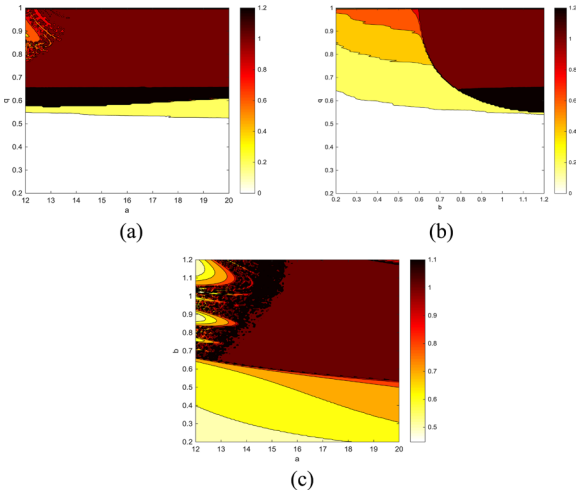

FIGURE 14. Dispersion entropy chromatogram.

From Figure 9 (b), Figure 11 (b), and Figure 13 (b), the complexity is the largest at the 0.6-order, especially compared with the 1-order complexity, so we can conclude that the complexity of the fractional-order Jafari-Sprott chaotic system is greater than the integer-order Jafari-Sprott chaotic system. The maximum complexity detected by using three types of entropy when system parameter a, b and order q changed is shown in Table 1.

TABLE 1. Comparison results of maximum complexity.

	Fuzzy entropy	Sample entropy	Dispersion entropy
a	0.009964	0.03686	1.14
b	0.01076	0.03324	1.106
q	0.06002	0.1994	1.249

According to Table 1, when using a single parameter as the independent variable, the complexity of the detection of dispersion entropy is larger than that of fuzzy entropy and sample entropy. In practical application, if the detection complexity is too small, it is not conducive to actual application.

By comparing the chromatograms in Figure 10, Figure 12, and Figure 14, we can obtain two conclusions:

1) Regardless of whether a, q, b, q or a, b are dual parameters, the color of the chromatogram of dispersion entropy is deeper than that of fuzzy entropy and sample entropy, which means that dispersion entropy can detect greater complexity not only under a single parameter, but also under the dual parameter.

2) By carefully observing the chromatograms of Figure 10, Figure 12, and Figure 14, it can be seen that dispersion entropy can detect areas where fuzzy entropy and sample entropy can not be detected, which means that the detection area of dispersion entropy is widest.

In summary, comparing two aspects of the detection complexity value size and the detection area size, it is concluded that in the complexity detection of the fractional- order Jafari-Sprott chaotic system, the detection performance of dispersion entropy is the best.

V. SYNCHRONOUS CONTROL OF FRACTIONAL-ORDER JAFARI-SPROTT CHAOTIC SYSTEM

A. SYNCHRONIZATION OF FRACTIONAL-ORDER JAFARI-SPROTT CHAOTIC SYSTEM BASED ON SLIDING MODE CONTROL

The mathematical model of the fractional-order Jafari-Sprott chaotic system is:

$$\begin{cases} D_{t_0}^q x_1 = x_2 \\ D_{t_0}^q x_2 = -x_1 + x_2 x_3 \\ D_{t_0}^q x_3 = -x_1 - a x_1 x_2 - b x_1 x_3 \end{cases} \tag{52}$$

Make (52) as the driving system, the response system is:

$$\begin{cases} D_{t_0}^q y_1 = y_2 \\ D_{t_0}^q y_2 = -y_1 + y_2 y_3 \\ D_{t_0}^q y_3 = -y_1 - a y_1 y_2 - b y_1 y_3 \end{cases} \tag{53}$$

The state error between the drive system and the response system is:

$$\begin{cases} e_1 = y_1 - x_1 \\ e_2 = y_2 - x_2 \\ e_3 = y_3 - x_3 \end{cases} \tag{54}$$

Then the state error between the drive system and the response system is:

$$\begin{cases} D_{t_0}^q e_1 = e_2 + u_1 \\ D_{t_0}^q e_2 = -e_1 - e_2 e_3 + e_2 y_3 + e_3 y_2 + u_2 \\ D_{t_0}^q e_3 = -e_1 + a(e_1 e_2 - e_1 y_2 - e_2 y_1) \\ +b(e_1 e_3 - e_1 y_3 - e_3 y_1) + u_3 \end{cases} \tag{55}$$

The control law design steps are as following:
Step 1: Introduce the fractional-order sliding mode surface.
Three fractional-order sliding mode surfaces is:

$$\begin{cases} s_1(t) = (D^q + \lambda_1) \int_0^t e_1(\tau) d\tau \\ s_2(t) = (D^q + \lambda_2) \int_0^t e_2(\tau) d\tau \\ s_3(t) = (D^q + \lambda_3) \int_0^t e_3(\tau) d\tau \end{cases} \tag{56}$$

The first-order derivative of the synovial surface is:

$$\begin{cases} \dot{s_1}(t) = D^q e_1(t) + \lambda_1 e_1(t) \\ \dot{s_2}(t) = D^q e_2(t) + \lambda_2 e_2(t) \\ \dot{s_3}(t) = D^q e_3(t) + \lambda_3 e_3(t) \end{cases} \tag{57}$$

When the error system moves on the synovial surface, $\dot{s_1}(t) = 0$ is satisfied. So the dynamic equation of the synovial surface is as follows:

$$\begin{cases} D^q e_1 = -\lambda_1 e_1 \\ D^q e_2 = -\lambda_2 e_2 \\ D^q e_3 = -\lambda_3 e_3 \end{cases} \tag{58}$$

Step 2: Design the control law.
Design the first Lyapunov function as:

$$V_1(t) = \frac{1}{2} s_1^2 \tag{59}$$

Its first-order derivative can be obtained:

$$\begin{aligned} \dot{V_1}(t) &= s_1 \dot{s_1} \\ &= s_1(D^q e_1 + \lambda_1 e_1) \\ &= s_1(e_2 + u_1 + \lambda_1 e_1) \end{aligned} \tag{60}$$

We can get $u_1 = -e_2 - \lambda_1 e_1 - k_1 sign(s_1)$.
Design the second Lyapunov function as:

$$V_2(t) = \frac{1}{2} s_2^2 \tag{61}$$

Its first-order derivative can be obtained:

$$\begin{aligned} \dot{V_2}(t) &= s_2 \dot{s_2} \\ &= s_2(D^q e_2 + \lambda_2 e_2) \\ &= s_2(-e_1 - e_2 e_3 + e_2 y_3 + e_3 y_2 + \lambda_2 e_2 + u_2) \end{aligned} \tag{62}$$

We can get $u_2 = e_1 + e_2 e_3 - e_2 y_3 - e_3 y_2 - \lambda_2 e_2 - k_2 sign(s_2)$.
Design the third Lyapunov function as:

$$V_3(t) = \frac{1}{2} s_3^2 \tag{63}$$

Its first-order derivative can be obtained:

$$\begin{aligned} \dot{V_3}(t) &= s_3 \dot{s_3} \\ &= s_3(D^q e_3 + \lambda_3 e_3) \\ &= s_3(-e_1 + a(e_1 e_2 - e_1 y_2 - e_2 y_1) \\ &\quad + b(e_1 e_3 - e_1 y_3 - e_3 y_1) + \lambda_3 e_3 + u_3) \end{aligned} \tag{64}$$

We can get:
$u_3 = e_1 - a e_1 e_2 + a e_1 y_2 + a e_2 y_1 - b e_1 e_3 + b e_1 y_3 + b e_3 y_1 - \lambda_3 e_3 - k_3 sign(s_3)$ where, $\lambda_1, \lambda_2, \lambda_3$ are synovial surface parameters, select $\lambda_1 = \lambda_2 = \lambda_3 = 4$, and k_1, k_2, k_3 are the gain of control law, select $k_1 = k_2 = k_3 = 1$.

The error graph between the drive and the corresponding system is shown in Figure 15.

From Figure 15, it can be seen that under the three control laws, the drive-response systems of fractional-order Jafari-Sprott chaotic system have completed synchronization, and the error tends to 0 with time, which illustrates the three control laws effectiveness and correctness.

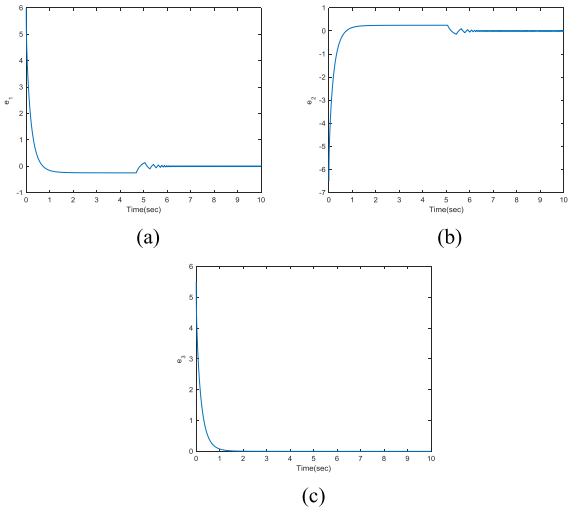

(a) (b) (c)

FIGURE 15. Synchronization error graph.

B. FRACTIONAL-ORDER JAFARI-SPROTT CHAOTIC SYSTEM CONTROL BASED ON FREQUENCY DISTRIBUTION MODEL OF FRACTIONAL-ORDER INTEGRAL OPERATOR

The mathematical model of the fractional-order Jafari-Sprott chaotic system is:

$$\begin{cases} D_{t_0}^q x_1 = x_2 \\ D_{t_0}^q x_2 = -x_1 + x_2 x_3 \\ D_{t_0}^q x_3 = -x_1 - a x_1 x_2 - b x_1 x_3 \end{cases} \tag{65}$$

Defining fractional-order systems $D^q x(t) = y(t)$, where $0 < q < 1$, it is equivalent to a linear continuous frequency distribution model [57]:

$$\begin{cases} \dfrac{\partial z(w,t)}{\partial t} = -wz(w,t) + y(t) \\ x(t) = \displaystyle\int_0^\infty \mu(w) z(w,t) dw \end{cases} \tag{66}$$

where, weight function $\mu(w) = \frac{\sin(q\pi)}{w^q \pi}$, system status $z(w,t) \in \mathbb{R}$.

The control law design steps are as follows:

Step 1: For the first equation in the mathematical model of the fractional-order Jafari-Sprott chaotic system, define the new coordinates as:

$$w_1 = x_1 \tag{67}$$

The dynamic equation of the first new coordinate is:

$$D_{t_0}^q w_1 = x_2 \tag{68}$$

According to the frequency distribution model of the fractional integral operator, Equation (68) is equivalent to the following equation:

$$\begin{cases} \dfrac{\partial z(w,t)}{\partial t} = -wz_1(w,t) + x_2 \\ w_1(t) = \displaystyle\int_0^\infty \mu(w) z_1(w,t) dw \end{cases} \tag{69}$$

Select Lyapunov function as:

$$V_1(t) = \frac{1}{2} \int_0^\infty \mu(w) z_1^2(w,t) dw \tag{70}$$

Its first-order derivative can be obtained:

$$\dot{V}_1(t) = \int_0^\infty \mu(w) z_1(w,t) \frac{\partial z(w,t)}{\partial t} dw \tag{71}$$

Take Equation (69) into Equation (71) to get:

$$\begin{aligned} \dot{V}_1(t) &= \int_0^\infty \mu(w) z_1(w,t)(-wz_1(w,t) + x_2) dw \\ &= -\int_0^\infty w\mu(w) z_1^2(w,t) dw + x_2 \int_0^\infty \mu(w) z_1(w,t) dw \\ &= -\int_0^\infty w\mu(w) z_1^2(w,t) dw + x_2 w_1 \\ &= -\int_0^\infty w\mu(w) z_1^2(w,t) dw - w_1^2 + w_1(x_1 + x_2) \end{aligned} \tag{72}$$

Step 2: Define the second new coordinate as:

$$w_2 = x_1 + x_2 \tag{73}$$

The dynamic equation of the second new coordinate is:

$$D_{t_0}^q w_2 = x_2 - x_1 + x_2 x_3 \tag{74}$$

According to the frequency distribution model of the fractional integral operator, Equation (74) is equivalent to the following equation:

$$\begin{cases} \dfrac{\partial z(w,t)}{\partial t} = -wz_2(w,t) + x_2 - x_1 + x_2 x_3 \\ w_2(t) = \displaystyle\int_0^\infty \mu(w) z_2(w,t) dw \end{cases} \tag{75}$$

Select Lyapunov function as:

$$V_2(t) = V_1(t) + \frac{1}{2} \int_0^\infty \mu(w) z_2^2(w,t) dw \tag{76}$$

Its first-order derivative can be obtained:

$$\dot{V}_2(t) = \dot{V}_1(t) + \int_0^\infty \mu(w) z_2(w,t) \frac{\partial z(w,t)}{\partial t} dw \tag{77}$$

By taking Equation (75) into Equation (77), we can get:

$$\dot{V}_2(t) = \dot{V}_1(t) + \int_0^\infty \mu(w) z_2(w,t) \frac{\partial z(w,t)}{\partial t} dw$$

$$
\begin{aligned}
&= \dot{V}_1(t) + \int_0^{\infty} \mu(w) z_2(w,t)[-w z_2(w,t) + x_2 - x_1 \\
&\quad + x_2 x_3]dw \\
&= \dot{V}_1(t) - \int_0^{\infty} w\mu(w) z_2^2(w,t)dw + (x_2 - x_1 + x_2 x_3) \\
&\quad \times \int_0^{\infty} \mu(w) z_2(w,t)dw \\
&= \dot{V}_1(t) - \int_0^{\infty} w\mu(w) z_2^2(w,t)dw + w_2(x_2 - x_1 + x_2 x_3) \\
&= -\int_0^{\infty} w\mu(w) z_1^2(w,t)dw - \int_0^{\infty} w\mu(w) z_2^2(w,t)dw - w_1^2 \\
&\quad + w_1(x_1 + x_2) + w_2(x_2 - x_1 + x_2 x_3) \\
&= -\int_0^{\infty} w\mu(w) z_1^2(w,t)dw - \int_0^{\infty} w\mu(w) z_2^2(w,t)dw - w_1^2 \\
&\quad - w_2^2 + w_2(x_1 + 2x_2 + x_2 x_3) \qquad (78)
\end{aligned}
$$

Step 3: Define the third new coordinate as:

$$w_3 = x_1 + 2x_2 + x_2 x_3 \qquad (79)$$

The dynamic equation of the third new coordinate is obtained:

$$
\begin{aligned}
D_{t_0}^q w_3 = {} & x_2 - 2x_1 + 2x_2 x_3 - x_1 x_3 - x_1 x_2 + x_2 x_3^2 \\
& - a x_1 x_2^2 - b x_1 x_2 x_3 + u \qquad (80)
\end{aligned}
$$

where, u is the required of control law. According to the frequency distribution model of the fractional integral operator, Equation (80) is equivalent to the following equation:

$$
\begin{cases}
\dfrac{\partial z(w,t)}{\partial t} = -w z_3(w,t) + x_2 - 2x_1 + 2x_2 x_3 - x_1 x_3 \\
-x_1 x_2 + x_2 x_3^2 - a x_1 x_2^2 - b x_1 x_2 x_3 + u \\
w_3(t) = \displaystyle\int_0^{\infty} \mu(w) z_3(w,t)dw
\end{cases} \qquad (81)
$$

Select Lyapunov function as:

$$\dot{V}_3(t) = \dot{V}_2(t) + \int_0^{\infty} \mu(w) z_3(w,t) \frac{\partial z(w,t)}{\partial t} dw \qquad (82)$$

Its first-order derivative can be obtained:

$$\dot{V}_3(t) = \dot{V}_2(t) + \int_0^{\infty} \mu(w) z_3(w,t) \frac{\partial z(w,t)}{\partial t} dw \qquad (83)$$

Take Equation (81) into Equation (83), we can get:

$$\dot{V}_3(t) = \dot{V}_2(t) + \int_0^{\infty} \mu(w) z_3(w,t) \frac{\partial z(w,t)}{\partial t} dw$$

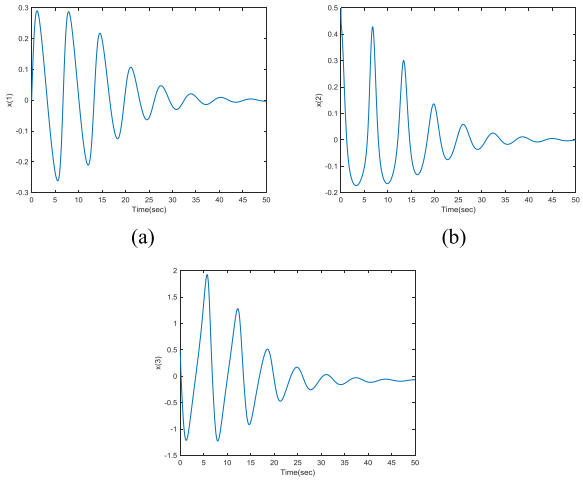

FIGURE 16. Control effect of each variable.

$$
\begin{aligned}
&= \dot{V}_2(t) + \int_0^{\infty} \mu(w) z_3(w,t)[-w z_3(w,t) + x_2 - 2x_1 \\
&\quad + 2x_2 x_3 - x_1 x_3 - x_1 x_2 + x_2 x_3^2 - a x_1 x_2^2 \\
&\quad - b x_1 x_2 x_3 + u]dw \\
&= \dot{V}_2(t) - \int_0^{\infty} w\mu(w) z_3^2(w,t)dw + (x_2 - 2x_1 + 2x_2 x_3 \\
&\quad - x_1 x_3 - x_1 x_2 + x_2 x_3^2 - a x_1 x_2^2 - b x_1 x_2 x_3 + u) \\
&\quad \times \int_0^{\infty} \mu(w) z_3(w,t)dw \\
&= \dot{V}_2(t) - \int_0^{\infty} w\mu(w) z_3^2(w,t)dw + w_3(x_2 - 2x_1 + 2x_2 x_3 \\
&\quad - x_1 x_3 - x_1 x_2 + x_2 x_3^2 - a x_1 x_2^2 - b x_1 x_2 x_3 + u) \\
&= -\int_0^{\infty} w\mu(w) z_1^2(w,t)dw - \int_0^{\infty} w\mu(w) z_2^2(w,t)dw \\
&\quad - \int_0^{\infty} w\mu(w) z_3^2(w,t)dw - w_1^2 - w_2^2 \\
&\quad + w_2(x_1 + 2x_2 + x_2 x_3) \\
&\quad + w_3(x_2 - 2x_1 + 2x_2 x_3 - x_1 x_3 - x_1 x_2 + x_2 x_3^2 \\
&\quad - a x_1 x_2^2 - b x_1 x_2 x_3 + u) \\
&= -\int_0^{\infty} w\mu(w) z_1^2(w,t)dw - \int_0^{\infty} w\mu(w) z_2^2(w,t)dw \\
&\quad - \int_0^{\infty} w\mu(w) z_3^2(w,t)dw - w_1^2 - w_2^2 - w_3^2 \\
&\quad + w_3(4x_2 + 3x_2 x_3 - x_1 x_2 - x_1 x_3 + x_2 x_3^2 - a x_1 x_2^2 \\
&\quad - b x_1 x_2 x_3 + u) \qquad (84)
\end{aligned}
$$

From Equation (84) we get the law of control $u = -4x_2 - 3x_2x_3 + x_1x_2 + x_1x_3 - x_2x_3^2 + ax_1x_2^2 + bx_1x_2x_3$, and the effect of each variable control is shown in Figure 16.

From Figure 16, we can see that under the action of the control law:

$$u = -4x_2 - 3x_2x_3 + x_1x_2 + x_1x_3 - x_2x_3^2 + ax_1x_2^2 + bx_1x_2x_3,$$

each state variable approaches, which illustrates the effectiveness and correctness of the design of the control law. Compared with other control methods, the control method based on the frequency distribution model of the fractional integral operator has the advantage that it only needs to design a control law to complete the control of each state variable.

VI. CONCLUSION

Based on the Adomian decomposition method, this paper combines fuzzy entropy algorithm, sample entropy algorithm, and dispersion entropy algorithm by comparing detection complexity value size and detection area size, and the dispersion entropy algorithm in analyzing the complexity of fractional-order Jafari-Sprott chaotic system is the best. In addition, the complexity of the fractional-order Jafari-Sprott chaotic system is greater than the integer-order Jafari-Sprott chaotic system, and the complexity is the highest especially at 0.6-order. Compared with the integer-order Jafari-Sprott chaotic system, the fractional-order Jafari-Sprott system has more research significance and it provides relevant theoretical basis for the application of fractional chaotic system in the fields of cryptography, confidential communication, and information security. Synchronization and control of fractional-order Jafari-Sprott chaotic system is accomplished by sliding model control and frequency distribution model of fractional-order integral operator respectively. In particular, the control effect of each variable is accomplished by designing a control law based on the frequency distribution model of fractional integral operator. The advantage of this method is that you only need to design a control law to complete the control of three state variables, at the same time the designed control law contains only state variables, and does not include integer or fractional order derivatives of state variables, so it is easy to implement. The system studied in the synchronization control in this paper is ideal, but in practice, many systems have external interference. How to complete the system's synchronous control in the presence of external interference is worthy of further study.

REFERENCES

[1] J. Horgan, "From complexity to perplexity," *Sci. Amer.*, vol. 272, no. 6, pp. 104–109, Jun. 1995.
[2] A. Lempel and J. Ziv, "On the complexity of finite sequences," *IEEE Trans. Inf. Theory*, vol. IT-22, no. 1, pp. 75–81, Jan. 1976.
[3] S. Pincus, "Approximate entropy (ApEn) as a complexity measure," *Chaos, Interdiscipl. J. Nonlinear Sci.*, vol. 5, no. 1, pp. 110–117, Mar. 1995.
[4] K. H. Sun, G. Q. Tan, and L. Y. Sheng, "The complexity analysis of TD-ERCS discrete chaotic pseudo-random sequences," *Acta Phys. Sinica*, vol. 57, no. 6, pp. 3359–3366, 2008.
[5] W. Chen, J. Zhuang, W. Yu, and Z. Wang, "Measuring complexity using FuzzyEn, ApEn, and SampEn," *Med. Eng. Phys.*, vol. 31, no. 1, pp. 61–68, Jan. 2009.
[6] K. H. Sun, S. B. He, L. Z. Yin, and A. Li-Kun, "Application of FuzzyEn algorithm to the analysis of complexity of chaotic sequence," *Acta Phys. Sinica*, vol. 61, no. 13, Jul. 2012, Art. no. 130507.
[7] H. A. Larrondo, C. M. González, M. T. Martín, A. Plastino, and O. A. Rosso, "Intensive statistical complexity measure of pseudorandom number generators," *Phys. A, Stat. Mech. Appl.*, vol. 356, no. 1, pp. 133–138, Oct. 2005.
[8] K. H. Sun, S. B. He, and L. Y. Sheng, "Complexity analysis of chaotic sequence based on the intensive statistical complexity algorithm," *Acta Phys. Sinica*, vol. 60, no. 2, 2011, Art. no. 020505.
[9] R. K. Azad, J. Subba Rao, and R. Ramaswamy, "Information-entropic analysis of chaotic time series: Determination of time-delays and dynamical coupling," *Chaos, Solitons Fractals*, vol. 14, no. 4, pp. 633–641, Sep. 2002.
[10] M. Sabeti, S. Katebi, and R. Boostani, "Entropy and complexity measures for EEG signal classification of schizophrenic and control participants," *Artif. Intell. Med.*, vol. 47, no. 3, pp. 263–274, Nov. 2009.
[11] A. Yildiz, M. Akin, M. Poyraz, and G. Kirbas, "Application of adaptive neuro-fuzzy inference system for vigilance level estimation by using wavelet-entropy feature extraction," *Expert Syst. Appl.*, vol. 36, no. 4, pp. 7390–7399, May 2009.
[12] F. Chen, J. Xu, F. Gu, X. Yu, X. Meng, and Z. Qiu, "Dynamic process of information transmission complexity in human brains," *Biol. Cybern.*, vol. 83, no. 4, pp. 355–366, Sep. 2000.
[13] F. S. Yang and W. C. Liao, "Approximate entropy: A complexity measure suitable for short data," *Chin. J. Med. Instrum.*, vol. 21, no. 5, pp. 283–286, 1997.
[14] D. E. Lake, J. S. Richman, M. P. Griffin, and J. R. Moorman, "Sample entropy analysis of neonatal heart rate variability," *Amer. J. Physiol.-Regulatory, Integrative Comparative Physiol.*, vol. 283, no. 3, pp. R789–R797, Sep. 2002.
[15] H. Liu, W. X. He, and X. P. Chen, "Approximate entropy and sample entropy for physiological time-series," *Chin. J. Sci. Instrum.*, vol. 25, no. 4, pp. 806–807 and 812, 2004.
[16] C. Yang, W. X. Xiao, Z. C. Chen, D. C. Wang, G. Chen, S. X. Tian, and S. H. Luo, "Research on EEG characteristics of sample entropy in depression patients," *J. Guilin Univ. Electron. Technol.*, vol. 34, no. 5, pp. 382–385, 2014.
[17] E. Ott, C. Grebogi, and J. A. Yorke, "Controlling chaos," *Phys. Rev. Lett.*, vol. 64, no. 11, pp. 1196–1199, 1990.
[18] L. M. Pecora, T. L. Carroll, G. A. Johnson, D. J. Mar, and J. F. Heagy, "Fundamentals of synchronization in chaotic systems, concepts, and applications," *Chaos, Interdiscipl. J. Nonlinear Sci.*, vol. 7, no. 4, pp. 520–543, Dec. 1997.
[19] T. L. Carroll and L. M. Pecora, "Driving nonlinear systems with chaotic signals," *Phys. Rev. A, Gen. Phys.*, vol. 1705, no. 1, pp. 22–32, 1992.
[20] M. T. Yassen, "Controlling chaos and synchronization for new chaotic system using linear feedback control," *Chaos, Solitons Fractals*, vol. 26, no. 3, pp. 913–920, Nov. 2005.
[21] C. H. Tao, J. A. Lu, and J. H. Lü, "The feedback synchronization of a unified chaotic system," *Acta Phys. Sinica*, vol. 51, no. 7, pp. 1497–1501, 2002.
[22] K. Pyragas, "Control of chaos via an unstable delayed feedback controller," *Phys. Rev. Lett.*, vol. 86, no. 11, pp. 2265–2268, Mar. 2001.
[23] J. Sun, "Some global synchronization criteria for coupled delay-systems via unidirectional linear error feedback approach," *Chaos, Solitons Fractals*, vol. 19, no. 4, pp. 789–794, Mar. 2004.
[24] J. Lü, T. Zhou, and S. Zhang, "Chaos synchronization between linearly coupled chaotic systems," *Chaos, Solitons Fractals*, vol. 14, no. 4, pp. 529–541, Sep. 2002.
[25] X. P. Guan, Z. P. Fan, H. P. Peng, and Y. Q. Wang, "The synchronization of chaotic systems based on RBF network in the presence of perturbation," *Acta Phys. Sinica*, vol. 50, no. 9, pp. 1670–1674, 2001.
[26] X. P. Guan, Y. G. Tang, Z. P. Fan, and Y. Q. Wang, "Neural network based robust adaptive synchronization of a chaotic system," *Acta Phys. Sinica*, vol. 50, no. 11, pp. 2112–2115, 2001.
[27] M. T. Yassen, "Adaptive chaos control and synchronization for uncertain new chaotic dynamical system," *Phys. Lett. A*, vol. 350, nos. 1–2, pp. 36–43, Jan. 2006.
[28] L. Guo-Hui, "An active control synchronization for two modified Chua circuits," *Chin. Phys.*, vol. 14, no. 3, pp. 472–475, Mar. 2005.

[29] U. E. Vincent, "Synchronization of Rikitake chaotic attractor using active control," *Phys. Lett. A*, vol. 343, nos. 1–3, pp. 133–138, Aug. 2005.
[30] L. Huang, R. Feng, and M. Wang, "Synchronization of uncertain chaotic systems with perturbation based on variable structure control," *Phys. Lett. A*, vol. 350, nos. 3–4, pp. 197–200, Feb. 2006.
[31] S. Etemadi, A. Alasty, and H. Salarieh, "Synchronization of chaotic systems with parameter uncertainties via variable structure control," *Phys. Lett. A*, vol. 357, no. 1, pp. 17–21, Aug. 2006.
[32] K.-Y. Lian, C.-S. Chiu, T.-S. Chiang, and P. Liu, "LMI-based fuzzy chaotic synchronization and communications," *IEEE Trans. Fuzzy Syst.*, vol. 9, no. 4, pp. 539–553, Aug. 2001.
[33] J. H. Kim, C.-W. Park, E. Kim, and M. Park, "Adaptive synchronization of T–S fuzzy chaotic systems with unknown parameters," *Chaos, Solitons Fractals*, vol. 24, no. 5, pp. 1353–1361, 2005.
[34] K. H. Sun, J. Mu, J. L. Zhou, and K. Zhong, "Synchronization control and its application for the unified chaotic system based on chaos observer," *Control Theory Appl.*, vol. 25, no. 4, pp. 794–798, 2008.
[35] F. Liu, Y. Ren, X. Shan, and Z. Qiu, "A linear feedback synchronization theorem for a class of chaotic systems," *Chaos, Solitons Fractals*, vol. 13, no. 4, pp. 723–730, Mar. 2002.
[36] D. Li, J.-A. Lu, and X. Wu, "Linearly coupled synchronization of the unified chaotic systems and the lorenz systems," *Chaos, Solitons Fractals*, vol. 23, no. 1, pp. 79–85, Jan. 2005.
[37] Y. Z. Liu and S. M. Fei, "Chaos synchronization between the Sprott-B and Sprott-C with linear coupling," *Acta Phys. Sinica*, vol. 55, no. 3, pp. 1035–1039, 2006.
[38] T. B. Wang and T. F. Qin, "Coupled synchronization of hyperchaotic systems," *Acta Phys. Sinica*, vol. 50, no. 10, pp. 1851–1855, 2001.
[39] B. X. Mao, "Self-adaptive sliding mode synchronization of fractional-order uncertainty Duffling systems based on a new reaching law," *Acta Scientiarum Naturalium Universitatis Sunyatseni*, vol. 56, no. 4, pp. 64–67, 2017.
[40] B. X. Mao and Q. L. Li, "Sliding mode chaos synchronization of a class of fractional-order Genesio-Tesi systems," *Acta Scientiarum Naturalium Universitatis Sunyatseni*, vol. 56, no. 2, pp. 76–79, 2017.
[41] P. Li and Z. Q. Zheng, "Sliding mode control approach with nonlinear integrator," *Control Theory Appl.*, vol. 28, no. 3, pp. 421–426, 2011.
[42] R. Y. Hou, Y. Li, and M. S. Hou, "A Proportional plus Integral Pursuit Guidance Law," *J. Northwestern Polytech. Univ.*, vol. 32, no. 2, pp. 303–308, 2014.
[43] R. P. Xu, M. M. Gao, and Z. Liu, "Sliding mode control of a new chaotic system," *J. Qingdao Univ., Natural Sci. Ed.*, vol. 25, no. 3, pp. 26–29, 2012.
[44] M. P. Aghababa and M. E. Akbari, "A chattering-free robust adaptive sliding mode controller for synchronization of two different chaotic systems with unknown uncertainties and external disturbances," *Appl. Math. Comput.*, vol. 218, no. 9, pp. 5757–5768, Jan. 2012.
[45] S. Song, B. Zhang, J. Xia, and Z. Zhang, "Adaptive backstepping hybrid fuzzy sliding mode control for uncertain fractional-order nonlinear systems based on finite-time scheme," *IEEE Trans. Syst., Man, Cybern., Syst.*, to be published, doi: 10.1109/TSMC.2018.2877042.
[46] S. Song, J. H. Park, B. Zhang, and X. Song, "Observer-based adaptive hybrid fuzzy resilient control for fractional-order nonlinear systems with time-varying delays and actuator failures," *IEEE Trans. Fuzzy Syst.*, to be published, doi: 10.1109/TFUZZ.2019.2955051.
[47] X. Y. Shu and S. J. Ma, "Dynamical behavior analysis and finite time synchronization of fractional order chaotic system without equilibrium point," *Sci. Technol. Eng.*, vol. 19, no. 31, pp. 34–41, 2019.
[48] K. Zhong, S. Gao, J. R. Huang, and F. C. Qian, "Robust adaptive synchronization control algorithm of fractional-order chaotic system with dual uncertainties," *Comput. Appl. Softw.*, vol. 36, no. 6, pp. 243–247, 2019.
[49] S. Jafari and J. C. Sprott, "Simple chaotic flows with a line equilibrium," *Chaos, Solitons Fractals*, vol. 57, pp. 79–84, Dec. 2013.
[50] X. Lü and G. T. Liu, "Comparison of several common fractional calculus definitions," *J. Inner Mongolia Normal Univ. Natural Sci. Ed.*, vol. 46, no. 4, pp. 479–482, 2017.
[51] L. X. Wei, H. Wang, and X. W. Mu, "Control of revolving inverted pendulum based on PSO-FOPID controller," *Control Eng. China*, vol. 26, no. 2, pp. 196–201, 2019.
[52] G. C. Zheng, C. X. Liu, and Y. Wang, "Dynamic analysis and finite time synchronization of a fractional-order chaotic system with hidden attractors," *Acta Phys. Sinica*, vol. 67, no. 5, 2018, Art. no. 050502.
[53] J. S. Duan, "Calculation of Adomian polynomials and its applications to integer-order and fractional order nonlinear differential equations," *Commun. Appl. Math. Comput.*, vol. 29, no. 2, pp. 187–210, 2015.
[54] P. Li, C. Y. Liu, L. P. Li, L. Z. Ji, S. Y. Yu, and C. C. Liu, "Multiscale multivariate fuzzy entropy analysis," *Acta Phys. Sinica*, vol. 62, no. 12, pp. 1–9, 2013.
[55] Y. J. Wang, H. L. Li, X. G. Tuo, and T. Shen, "A denoising method for microseismic signal based on the ensemble empirical mode decomposition of sample entropy threshold," *Geophys. Geochem. Explor.*, vol. 43, no. 5, pp. 1083–1089, 2019.
[56] H. Azami and J. Escudero, "Coarse-graining approaches in univariate multiscale sample and dispersion entropy," *Entropy*, vol. 20, no. 2, p. 138, 2018.
[57] Y. H. Wei, "Adaptive control for uncertain fractional order systems," Ph.D. dissertation, Univ. Sci. Technol. China, Hefei, China, 2015.

GUOHUI LI received the bachelor's degree in electronic information engineering from the Chongqing University of Technology, Chongqing, China, in 2001, the master's degree in circuit and system from the University of Electronic Science and Technology of China, Chengdu, China, in 2004, and the Ph.D. degree in acoustics from Northwestern Polytechnical University, Xi'an, China, in 2015. He is currently an Associate Professor with the School of Electronic Engineering, Xi'an University of Posts and Telecommunications, Shaanxi, China. His research interests include underwater acoustic signal processing and chaotic signal processing.

XIANGYU ZHANG received the bachelor's degree in measurement and control technology and instruments from the Baoji College of Arts and Sciences, Baoji, Shaanxi, China, in 2018. He is currently pursuing the master's degree in electronics and communication engineering with the Xi'an University of Posts and Telecommunications, Xi'an, Shaanxi. His research interests include characteristics of fractional-order chaotic systems and synchronization control.

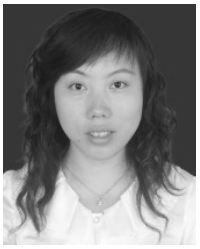

HONG YANG received the bachelor's and master's degrees in mechanical and electronic engineering from the University of Electronic Science and Technology of China, Chengdu, China, in 2003 and 2006, respectively, and the Ph.D. degree in acoustics from Northwestern Polytechnical University, Xi'an, Shaanxi, China, in 2015. She is currently an Associate Professor with the School of Electronic Engineering, Xi'an University of Posts and Telecommunications, Shaanxi. Her research interests include underwater acoustic signal processing and chaotic signal processing.